

Liquid Propellant Migration Control for a Teardrop Tank System

Masahiko Utsumi*

Ishikawajima–Harima Heavy Industries Company, Ltd., Yokohama 235-0001, Japan

The use of pressurized gas as a means to control liquid propellant migration in a teardrop tank system subjected to rotational unbalance caused by the detachment of an object from a spinning satellite is investigated. The effectiveness of this control method is ascertained by numerical computation that predicts the stationary position of the liquid propellant in the tank system. A multiloop iteration algorithm is developed to satisfy a continuity condition for the liquid pressure in the pipes connecting the tanks and to determine the position of the center of mass of the whole satellite–liquid system. Numerical results show that the critical total propellant mass below which some of the tanks empty can be controlled to a very small value by increasing the gas pressure, whereas the tilt of the principle inertia axis is reduced to about 50% level of its uncontrolled value by moderate gas pressure and is kept constant with the further increase in the gas pressure.

Nomenclature

a	= radius of spherical part of tanks (Fig. 1), m
G	= center of mass of satellite–liquid system
g	= gravity acceleration due to vehicle propulsion, m/s^2
H	= distance between x_{1i} axis and top of conical part of tank (Fig. 1), m
i	= tank number
L	= distance between z axis and top of conical part of tank (Fig. 1), m
M_f	= total propellant mass in tank system, kg
$M_{f,cr}$	= critical total propellant mass, kg
M_{fi}	= propellant mass in tank i , kg
n	= polytropic index
p_{gi}	= gas pressure in tank i , N/m^2
p_{g0}	= gas pressure initially supplied when valves among tanks are open, N/m^2
p_i	= liquid pressure in tank i , N/m^2
$(R_i, \theta_i, \varphi_i)$	= spherical coordinates for tank i
v_{gi}	= volume of gas in tank i , m^3
v_i	= volume of each tank, m^3
(x, y, z)	= coordinates fixed to spinning satellite (Fig. 1a), m
$(x_{fGi}, y_{fGi}, z_{fGi})$	= (x, y, z) coordinates of the center of mass of propellant in tank i , m
(x_G, y_G, z_G)	= (x, y, z) coordinates of the center of mass of satellite–liquid system, m
(x_{1i}, y_{1i}, z_{1i})	= coordinates for tank i (Fig. 1), m
(x_{2i}, y_{2i}, z_{2i})	= coordinates for tank i (where z_{2i} is the tank axis; Fig. 1b), m
z	= geometrical centerline of tank system (Fig. 1)
α_i	= circumferential coordinate of tank i measured from x axis (Fig. 1a)
γ	= angle between tank axis z_{2i} and $-z$ direction (Fig. 1b)
θ_C	= half the apex angle of conical part of the tanks (Fig. 1b)
θ_{tilt}	= tilt of principal inertia axis of satellite–liquid system from the z direction

(ξ, η, ζ)	= coordinates fixed to the spinning satellite (Fig. 1), m
ρ	= density of liquid propellant, kg/m^3
Ω	= angular velocity of spin, rad/s

Subscripts

f	= fluid (liquid propellant)
i	= tank number
r	= rigid body (main body of satellite and objects to be detached)

Introduction

FOR a spin-stabilized satellite, a teardrop tank system as shown in Fig. 1 is widely used. The teardrop-shaped form of the tanks is given by spherical and conical surfaces and arranged in circumferential 120-deg pitch. Each tank is tilted to hold the liquid propellant at the outlet for it (the top of the conical surface) by using centrifugal force due to spinning and gravity force caused by the acceleration of the vehicle propulsion.

When rotational unbalance is not present, the teardrop tank system spins around its geometrical centerline z and the propellant is distributed equally over the three tanks. However, when rotational unbalance is caused due to the detachment of objects from the main body of the satellite, the center of mass of the satellite–liquid system largely displaces from its original position and the propellant migrates among tanks. As a result of this, the liquid propellant masses of the three tanks are not equal to each other and the following problems are caused: 1) Some of the tanks become empty and suction of gas into the engine propulsion system is caused. 2) The tilt of the principal inertia axis of the system from the centerline of the main body becomes large. Investigations regarding a solution to these problems are relatively scarce, although several papers exist concerned with the determination of the liquid position in a teardrop tank system^{1,2} and a tank with a propellant management device.^{3–6} In a previous paper,⁷ it was shown that the foregoing problems can be solved by moving some of the tanks outward in such a manner that the distances of the tanks from the center of mass of the whole satellite–liquid system are approximately equal. However, this method requires space and apparatus for moving the tanks. Furthermore, the tank motion may cause sloshing, which is an unfavorable oscillatory disturbance to the attitude control of the satellite. This paper proposes a more cost-efficient and securer propellant migration control method and ascertains the effectiveness of the proposed method by numerical computation. The proposed method supplies pressurized gas to the ullage of each tank and confines the gas by closing the valves among the tanks. The numerical computation conducted in the present study requires more complex iterative procedures than the analysis presented in the previous paper.⁷ This is not only because the position of the center of mass

Received 3 August 2005; revision received 14 November 2005; accepted for publication 14 November 2005. Copyright © 2006 by the American Institute of Aeronautics and Astronautics, Inc. All rights reserved. Copies of this paper may be made for personal or internal use, on condition that the copier pay the \$10.00 per-copy fee to the Copyright Clearance Center, Inc., 222 Rosewood Drive, Danvers, MA 01923; include the code 0022-4650/06 \$10.00 in correspondence with the CCC.

*Associate Manager, Machine Element Department, Technical Research Laboratory, 1 Shin-nakaharacho, Isogo-ku; masahiko_utsumi@ihi.co.jp.

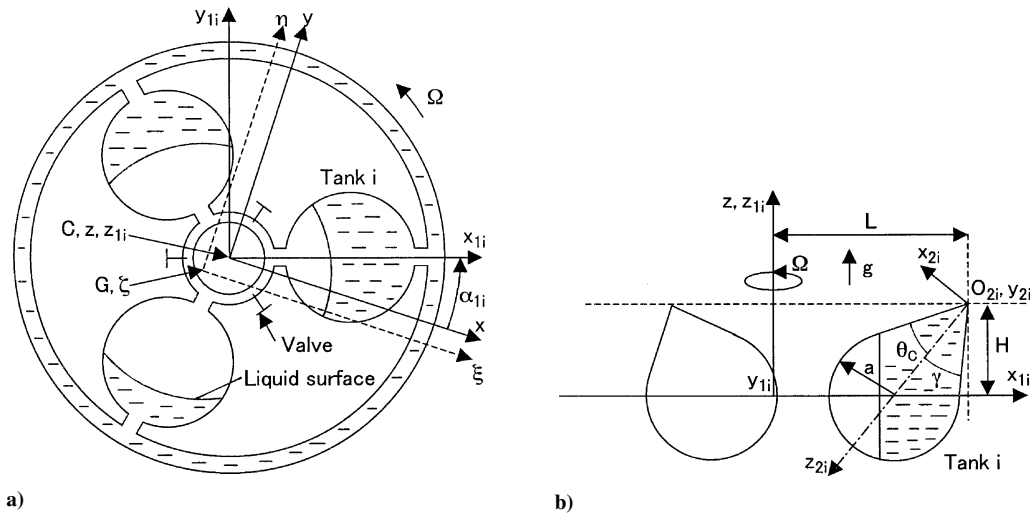


Fig. 1 Teardrop tank system and coordinate systems.

of the whole satellite–liquid system cannot be prescribed, but also because the integration constant appearing in the pressure equation must be defined for each tank and each integration constant must be determined from a continuity condition for the liquid pressure in the pipes connecting the tanks. Numerical results illustrate controlling effects of the gas pressure on the critical total propellant mass, below which some of the tanks empty, and on the tilt of the principle inertia axis.

Analysis

Cartesian Coordinate Systems

In Fig. 1, $Cxyz$ is a rotating coordinate system fixed to the satellite. The z axis is the geometrical centerline of the tank system. The circumferential position of the center of the spherical part of each tank i is prescribed by the angle α_i measured from the x axis. When rotational unbalance is caused by detachment of an object from the satellite, the center of mass of the system represented by G in Fig. 1 moves from its original position on the z axis so that the system spins around another axis, for example, the ζ axis, which passes through G . As a result, the propellant migrates among the tanks and the liquid propellant masses of the three tanks are not equal to each other, as shown in Fig. 1. A practical example of the unbalance will be given in the section for numerical results. This paper considers the case in which the z coordinates of the centers of mass of all of the components of the system, that is, the main body of the satellite without propellant, the object to be detached, and the propellant, are close to 0. Thus, the z component of the displacement vector of the center of mass G from its original position is small. Such a case is common and favorable for the sake of weight balancing and allows us to make the approximation that the z axis is parallel to the ζ axis. We express the relation between the coordinate systems $Cxyz$ and $G\xi\eta\zeta$ as

$$\begin{Bmatrix} \xi \\ \eta \\ \zeta \end{Bmatrix} = \begin{Bmatrix} x - x_G \\ y - y_G \\ z - z_G \end{Bmatrix} \quad (1)$$

Note that the x , y , and z coordinates of the center of the mass G are determined from iterative computation explained in the next section because the position of G is unknown or cannot be prescribed.

For each tank i , where $i = 1-3$, the following two coordinate systems are introduced: First, as shown in Fig. 1a, we define $Cx_1iy_1iz_1i$ by rotating $Cxyz$, the angle α_i , around the z axis:

$$\begin{Bmatrix} x \\ y \\ z \end{Bmatrix} = \begin{bmatrix} \cos \alpha_i & -\sin \alpha_i & 0 \\ \sin \alpha_i & \cos \alpha_i & 0 \\ 0 & 0 & 1 \end{bmatrix} \begin{Bmatrix} x_{1i} \\ y_{1i} \\ z_{1i} \end{Bmatrix} \quad (2)$$

Second, as shown in Fig. 1b, we set $O_{2i}x_{2i}y_{2i}z_{2i}$ by rotating $Cx_1iy_1iz_1i$, the angle $\pi - \gamma$, around the y_{1i} axis and shifting the origin to the top of the conical surface of the tank:

$$\begin{Bmatrix} x_{1i} \\ y_{1i} \\ z_{1i} \end{Bmatrix} = \begin{bmatrix} -\cos \gamma & 0 & -\sin \gamma \\ 0 & 1 & 0 \\ \sin \gamma & 0 & -\cos \gamma \end{bmatrix} \begin{Bmatrix} x_{2i} \\ y_{2i} \\ z_{2i} \end{Bmatrix} + \begin{Bmatrix} L \\ 0 \\ H \end{Bmatrix} \quad (3)$$

where z_{2i} is the centerline of the tank and is in the plane $y_{1i} = 0$.

Spherical Coordinates

The analysis to be conducted for the verification of the proposed propellant migration control method requires volume integrations for calculating the mass, the coordinates of the center of mass, and the inertia tensors of the liquid in each tank. These volume integrations become considerably complex due to the presence of the conical parts of the tanks and the curvatures of the circular cylindrical liquid surfaces. Therefore, the teardrop tanks were approximated by the spherical tanks of radius a by neglecting the conical parts, and the liquid surfaces were approximated as planes in conventional studies. However, in the practical example here, taking into account the presence of the conical parts is obligatory to avoid underestimating the tilt of the principal inertia axis as is illustrated in the numerical computation to come, and the curvatures of the circular cylindrical liquid surfaces should be taken into account because the tanks are confined in the satellite compactly and are close to each other. To conduct the volume integrations successfully, spherical coordinates $(R_i, \theta_i, \varphi_i)$ are introduced, whose origin is at the intersection of the spherical surface of tank i and the tank axis z_{2i} , that is,

$$\begin{aligned} x_{2i} &= R_i \sin \theta_i \cos \varphi_i, & y_{2i} &= R_i \sin \theta_i \sin \varphi_i \\ z_{2i} &= a + a/\sin \theta_c - R_i \cos \theta_i \end{aligned} \quad (4)$$

In terms of these spherical coordinates, the mass, the coordinates of the center of mass, and the inertia tensors of the liquid in tank i can be expressed as

$$M_{fi} = \rho \int_0^{2\pi} \int_0^{\theta_{i,\max}(\varphi_i)} \int_{R_{iM}(\theta_i, \varphi_i)}^{R_{iW}(\theta_i)} R_i^2 \sin \theta_i dR_i d\theta_i d\varphi_i \quad (5)$$

$$\begin{Bmatrix} x_{fGi} \\ y_{fGi} \\ z_{fGi} \end{Bmatrix} = \frac{\rho}{M_{fi}} \int_0^{2\pi} \int_0^{\theta_{i,\max}(\varphi_i)} \int_{R_{iM}(\theta_i, \varphi_i)}^{R_{iW}(\theta_i)} \begin{Bmatrix} \xi + x_G \\ \eta + y_G \\ \zeta + z_G \end{Bmatrix} \times R_i^2 \sin \theta_i dR_i d\theta_i d\varphi_i \quad (6)$$

$$\begin{pmatrix} I_{fi,\xi\xi} \\ I_{fi,\eta\eta} \\ I_{fi,\zeta\zeta} \\ I_{fi,\xi\eta} \\ I_{fi,\eta\zeta} \\ I_{fi,\zeta\xi} \end{pmatrix} = \rho \int_0^{2\pi} \int_0^{\theta_{i,\max}(\varphi_i)} \int_{R_{iM}(\theta_i, \varphi_i)}^{R_{iW}(\theta_i)} \begin{pmatrix} \eta^2 + \zeta^2 \\ \zeta^2 + \xi^2 \\ \xi^2 + \eta^2 \\ \xi\eta \\ \eta\zeta \\ \zeta\xi \end{pmatrix} \times R_i^2 \sin \theta_i dR_i d\theta_i d\varphi_i \quad (7)$$

where $R_{iM}(\theta_i, \varphi_i)$ and $R_{iW}(\varphi_i)$ are the R_i coordinates of the liquid surface and the tank wall, respectively, and $\theta_{i,\max}(\varphi_i)$ is the θ_i coordinate of the contact line of the liquid surface with the tank wall. These functions' forms are determined by hand calculations. The variables (ξ, η, ζ) in Eqs. (6) and (7) can be expressed in terms of $(R_i, \theta_i, \varphi_i)$ by using Eqs. (1–4).

Iterative Computation Procedures

At the initial stage, rotational unbalance is not present and the valves are open. Let us represent the gas pressure and propellant mass supplied to each tank at this stage by p_{g0} and $M_f/3$, respectively, where M_f represents the total propellant mass. When rotational unbalance is produced by detachment of an object, the valves are closed to control the migration of the liquid propellant. The stationary position of the liquid propellant for this unbalanced case is determined by the following iterative computation procedures.

In step 1, under an assumed position G_{old} of the center of mass, we derive the following basic equations:

$$\frac{1}{\rho} \frac{\partial p_i}{\partial \xi} = \Omega^2 \xi \quad (8a)$$

$$\frac{1}{\rho} \frac{\partial p_i}{\partial \eta} = \Omega^2 \eta \quad (8b)$$

$$\frac{1}{\rho} \frac{\partial p_i}{\partial \zeta} = g \quad (8c)$$

where Eqs. (8a) and (8b) correspond to the equilibrium conditions between the pressure gradient and the centrifugal force, whereas Eq. (8c) corresponds to the equilibrium between the pressure gradient and the gravity force. These equations can be derived from the Navier–Stokes equation by neglecting the fluid velocity components. Integrating Eqs. (8a–8c), we obtain

$$p_i = \rho g \zeta + \frac{1}{2} \rho \Omega^2 (\xi^2 + \eta^2) + C_i \quad (9)$$

where C_i is the integration constant for tank i . Note that when the valves are closed, this integration constant must be defined for each tank i .

In step 2, we assume the propellant mass M_{fi} in each tank i . Calculate the corresponding gas volume v_{gi} and gas pressure p_{gi} in each tank by

$$v_{gi} = v_i - \rho^{-1} M_{fi} \quad (10)$$

$$p_{gi} = p_{g0} (v_i - \rho^{-1} \frac{1}{3} M_f)^n / v_{gi}^n \quad (11)$$

where v_i is the volume of the tank and n is the polytropic index.

In step 3, by using the condition that the liquid pressure p_i at the liquid surface is equal to the gas pressure p_{gi} , we determine the liquid surface shape as

$$\zeta = (-\Omega^2/2g)(\xi^2 + \eta^2) + (1/\rho g)(p_{gi} - C_i) \quad (12)$$

In step 4, we determine the integration constant C_i through iterative computation such that the liquid mass corresponding to the liquid surface equation (12) coincides with the liquid mass M_{fi} assumed in step 2.

In step 5, we check whether the determined integration constants C_i for the three tanks are equal. This condition indicates that the

liquid pressure is continuous in the pipes connecting each tank because, for arbitrary places in the pipes, the values of ξ , η , and ζ in Eq. (9) are commonly defined. This condition cannot be satisfied by M_{fi} assumed in step 2. To satisfy this condition, change the assumed value of M_{fi} and repeat the procedures from step 2. Thus, we determine the accurate values of M_{fi} , p_{gi} , and C_i for the position of the center of mass assumed in step 1. When the valves are open, as in the case considered in the previous paper,⁷ the integration constant appearing in the liquid pressure equation may be defined commonly for each tank and can be determined from the condition that the total liquid mass contained in tanks 1–3 equals the prescribed value of M_f . However, for the problem under consideration here, the integration constant in the pressure equation is defined for each tank and is determined by adjusting the mass of liquid in each tank such that the continuity condition for the liquid pressure in the pipes connecting the tanks is satisfied.

In, step 6, using the position of the liquid surface in each tank determined by Eq. (12), we estimate the position of the center of mass G of the whole satellite–liquid system.

In step 7, we check whether this calculated center of mass G_{new} coincides with G_{old} initially assumed in step 1. This coincidence cannot be satisfied because, for the propellant migration problem, the required position of the center of mass of the whole satellite–liquid system is unknown or cannot be prescribed. To achieve the coincidence, adjust the assumed position G_{old} and repeat the procedures from step 1.

These steps are summarized in Fig. 2.

Numerical Results

The numerical calculation is conducted for the following parameters: $\rho = 1009 \text{ kg/m}^3$, $\Omega = 4\pi \text{ rad/s}$ (120 rpm), $g = 0.5 \text{ m/s}^2$, $a = 0.24 \text{ m}$, $\theta_C = 40^\circ$, $\gamma = 42^\circ$, $L = 0.550 \text{ m}$, and $H = 0.278 \text{ m}$. In this case, the center of the spherical surface of each tank is 0.3 m away from the z axis and lies in the plane $z = 0$. The gravity g is chosen to be an arbitrary value for which the liquid surface becomes cylindrical. This corresponds to the part of mission just before the detachment. The circumferential coordinates of the tanks are $\alpha_1 = 210^\circ$, $\alpha_2 = 90^\circ$, and $\alpha_3 = -30^\circ$ (Fig. 3).

The mass and inertia tensors of the main body of the satellite without liquid propellant are, respectively, $M_{r0} = 200 \text{ kg}$, $I_{r0xx} = I_{r0yy} = 60 \text{ kg} \cdot \text{m}^2$, $I_{r0zz} = 80 \text{ kg} \cdot \text{m}^2$, and $I_{r0xy} = I_{r0yz} = I_{r0zx} = 0$. The center of mass is at $x = y = z = 0$.

The common mass of the objects j that are to be detached, $j = 1, 2$ (Fig. 3), is $M_{rj} = 40 \text{ kg}$. As shown in Fig. 3, the centers of mass of objects 1 and 2 are located at 30° and 210° deg, respectively, in the circumferential direction measured from the x axis. These centers of mass are on the circle $(x^2 + y^2)^{1/2} = 0.85 \text{ m}$ in the plane $z = 0$. The common inertia tensors of each object around its principal inertia axes α , β , and γ that are parallel to the x , y , and z axes, respectively, are $I_{rj\alpha\alpha} = I_{rj\beta\beta} = 4 \text{ kg} \cdot \text{m}^2$, $I_{rj\gamma\gamma} = 0.4 \text{ kg} \cdot \text{m}^2$, and $I_{rj\alpha\beta} = I_{rj\beta\gamma} = I_{rj\gamma\alpha} = 0$.

In this example, the propellant is hydrazine. Its surface tension T is 0.0725 N/m . The rotational Bond number defined by $Bo = \rho a^3 \Omega^2 / T$ is equal to 30,381 and is sufficiently large. Hence, we can confidently neglect capillary effects.

First, the numerical calculation is conducted for the case where object 1 is detached, object 2 is retained, and the propellant migration is not controlled, that is, $p_{g0} = 0$. The results are shown in Figs. 4a–4d. These results for $p_{g0} = 0$ and discussions of them are necessary to confirm the effectiveness of the propellant migration control method presented in this paper.

Figures 4a and 4b show the x_G coordinate of the center of mass for the whole satellite–liquid system and the propellant masses M_{fi} in tanks i , where $i = 1$ –3, respectively, as functions of the total propellant mass

$$M_f = \sum_{i=1}^3 M_{fi}$$

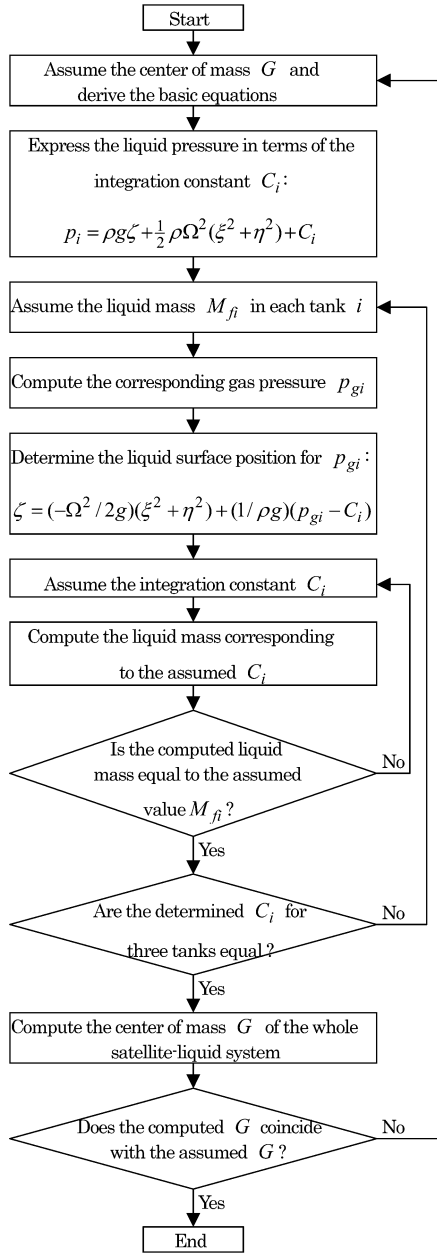


Fig. 2 Iterative computation procedures.

Because of the symmetry of the problem about the plane $y = x/\sqrt{3}$, the relations $y_G = x_G/\sqrt{3}$ and $M_{f2} = M_{f3}$ are satisfied. It can be seen that because the displacement of G from its original position is not negligibly small compared to the tank size (Fig. 4a), unbalance between M_{f1} and M_{f2} is large, and tank 1, which is nearest to G , empties when the total propellant mass M_f is smaller than the fairly large critical value $M_{f,cr} = 37$ kg (Fig. 4b).

Figure 4c shows the tilt θ_{ilt} of the principal inertia axis from the z direction. This can be calculated from the eigenvectors of the inertia tensor matrix for the whole satellite-liquid system. It can be seen from Fig. 4c that θ_{ilt} does not decrease monotonically with the decrease of the total propellant mass M_f but exhibits a maximum near the critical total propellant mass $M_{f,cr}$. This variation of the tilt is explained by the difference between z_{fG1} and $z_{fG2}(=z_{fG3})$ shown in Fig. 4d as follows: Divide the liquid domain in each tank into the spherical part $x_{2i}^2 + y_{2i}^2 + [z_{2i} - (a/\sin\theta_C)]^2 \leq a^2$ and the remaining conical part. As M_f increases, the propellant in the spherical part becomes more and more predominant while keeping its center of mass in the plane $z = 0$ irrespective of M_f because the liquid surface is circular cylindrical in the present case. Therefore, for large M_f , each value of z_{fGi} , $i = 1-3$, is close to 0, as

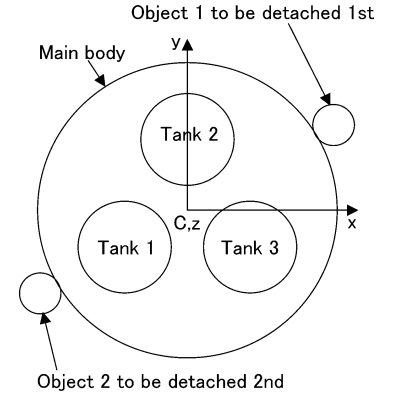


Fig. 3 Numerical example.

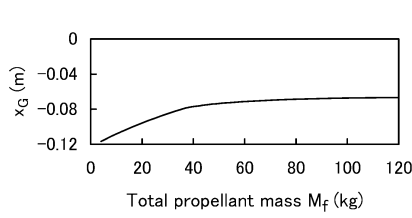
shown in Fig. 4d. In addition, this example considers the standard case where the z coordinates of the main body and object 2 that have not yet been detached are 0. Hence, θ_{ilt} is small for large M_f . On the other hand, when M_f is decreased, z_{fG1} and $z_{fG2}(=z_{fG3})$ shown in Fig. 4d rise up more sensitively depending on the decrease in M_f because of the relative importance of the propellant outside the spherical part and exhibit the remarkable difference due to the large difference between M_{f1} and $M_{f2}(=M_{f3})$. Therefore, θ_{ilt} exhibits a maximum near the critical total propellant mass $M_{f,cr}$ before tending to zero for $M_f \rightarrow 0$.

The foregoing discussion indicates that not only the large $M_{f,cr}$ but also the maximum θ_{ilt} is due to the difference between M_{f1} and $M_{f2}(=M_{f3})$. Therefore, $M_{f,cr}$ and θ_{ilt} can be simultaneously reduced by the proposed propellant migration control method. Figure 5 shows the numerical results for the case where pressurized gas is supplied to the ullage of each tank and is confined in each tank by closing the valves among the tanks. It can be confirmed from Fig. 5 that 1) although a large displacement of the center of mass is caused (Fig. 5a) the critical total propellant mass can be decreased markedly (Fig. 5b) and 2) θ_{ilt} can be controlled to a smaller value (Fig. 5c) because the difference between z_{fG1} and $z_{fG2}(=z_{fG3})$ can be reduced (Fig. 5d) in contrast to the earlier case of $p_{g0} = 0$.

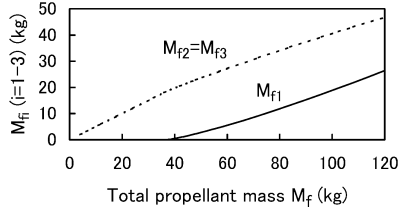
Figure 6 shows the influence of the initial gas pressure p_{g0} on the critical total propellant mass $M_{f,cr}$. It can be seen that $M_{f,cr}$ can be reduced to a certain extent even by not so large p_{g0} . However, to make $M_{f,cr}$ very small, for example, 2 kg, thereby achieving good propellant consumption efficiency, high initial gas pressure is required. For this reason, a large value of p_{g0} has been employed in the earlier numerical example presented in Fig. 5. The dotted curve in Fig. 6 shows the critical total propellant mass for the case where polytropic index n is reduced to 1. In this case, $M_{f,cr}$ increases considerably and more propellant is left unused unless p_{g0} is sufficiently large because the propellant migration control effect becomes weak. Therefore, to keep the increase in $M_{f,cr}$ against the reduction of the polytropic index n very small, a large value of p_{g0} is required.

Figure 7 shows the influence of the initial gas pressure p_{g0} on the maximum value of θ_{ilt} . It can be seen that the maximum value of θ_{ilt} can be reduced to about 50% level of its uncontrolled value by a not very high gas pressure. However, it is kept constant with the further increase in the gas pressure in contrast to the critical total propellant mass $M_{f,cr}$ shown in Fig. 6. This trend signifies that the control effect achieved for θ_{ilt} is limited due to the presence of the conical parts of the teardrop tanks. If these conical parts are neglected and the teardrop tanks are approximated by the spherical tanks as in conventional studies, the difference between z_{fG1} and $z_{fG2}(=z_{fG3})$ vanishes and all z_{fGi} , $i = 1-3$, are reduced to small values for all values of M_f , so that θ_{ilt} is underestimated as is shown in Fig. 8. Therefore, to not underestimate θ_{ilt} , it is essential to take into account the exact shape of the teardrop tanks. For such an exact treatment, the spherical coordinates introduced by Eq. (4) are helpful.

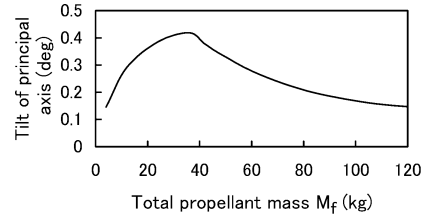
Let us approximately estimate the stress σ that arises in the tank wall. For the case of $p_{g0} = 1.57 \times 10^6$ N/m², the propellant migration is effectively controlled and the change in the propellant volume in each tank is small. Therefore, the variation in the gas pressure



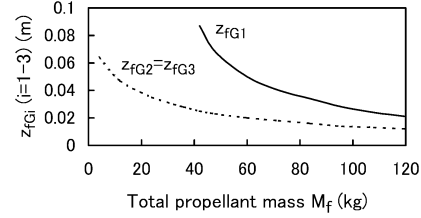
a) The x coordinate x_G of center of mass for whole satellite-liquid system



b) Propellant masses M_{fi} in tanks i , where $i = 1, 2, 3$

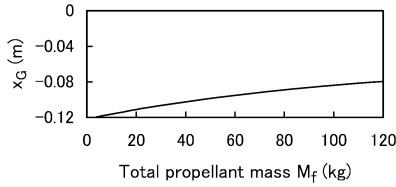


c) Tilt θ_{tilt} of principal inertia axis from z direction

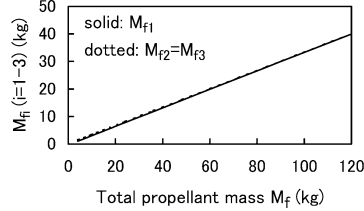


d) The z coordinates z_{fGi} of the centers of mass for propellant in tanks i , where $i = 1, 2, 3$

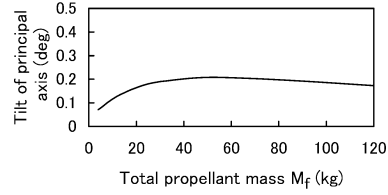
Fig. 4 Numerical results for the case in which $p_{g0} = 0$.



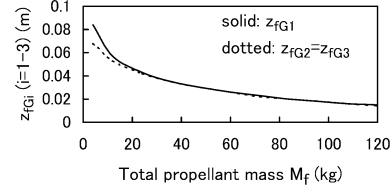
a) The x coordinate x_G of center of mass for whole satellite-liquid system



b) Propellant masses M_{fi} in tanks i , where $i = 1, 2, 3$



c) Tilt θ_{tilt} of principal inertia axis from z direction



d) The z coordinates z_{fGi} of centers of mass for propellant in tanks i , where $i = 1, 2, 3$

Fig. 5 Numerical results for the case in which $p_{g0} = 1.57 \times 10^6 \text{ N/m}^2$ and $n = 1.3$.

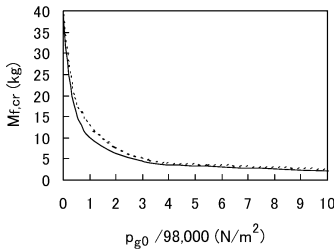


Fig. 6 Influence of initial gas pressure on critical total propellant mass: —, $n = 1.3$ and \cdots , $n = 1.0$.

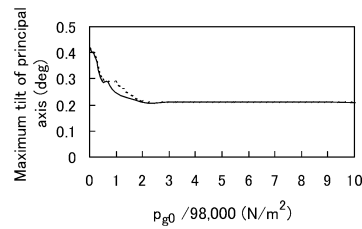


Fig. 7 Influence of the initial gas pressure on the maximum tilt of the principal inertia axis: —, $n = 1.3$ and \cdots , $n = 1.0$.

p_{gi} in each tank from its initial value p_{g0} is small. From Eq. (12), the liquid surface position $(\xi, \eta) = (\xi_M, \eta_M)$ for a certain value of ζ satisfies

$$\zeta = (-\Omega^2/2g)(\xi_M^2 + \eta_M^2) + (1/\rho g)(p_{gi} - C_i) \quad (13)$$

Eliminating C_i from Eqs. (9) and (13), we obtain

$$p_i = p_{gi} + (\rho\Omega^2/2)(\xi^2 + \eta^2) - (\rho\Omega^2/2)(\xi_M^2 + \eta_M^2) \quad (14)$$

The maximum of the difference between the values of $\frac{1}{2}\rho\Omega^2(\xi^2 + \eta^2)$ in the liquid domain and on the liquid surface is roughly $2 \times 10^4 \text{ N/m}^2$, which is much smaller than $p_{g0} = 1.57 \times 10^6$

N/m^2 . The first term p_{gi} on the right-hand side of Eq. (14) is close to p_{g0} , as mentioned earlier. For these reasons, we are allowed to evaluate approximately the stress σ arising in the tank wall by $p_{g0}a/2t$, where t is the thickness of the wall. The tanks' material, thickness, and size are selected such that this stress does not exceed the admissible value.

It can be seen from Figs. 4a and 5a that the distance of the center of mass of the whole satellite-liquid system from its original position is decreased when the total propellant mass M_f is increased. This trend indicates that the position of the center of mass is restored due to the presence of the liquid propellant. Furthermore, the following two significant observations can be made from Figs. 4a and 5a: 1) This restoring effect is stronger for $p_{g0} = 0$ than for

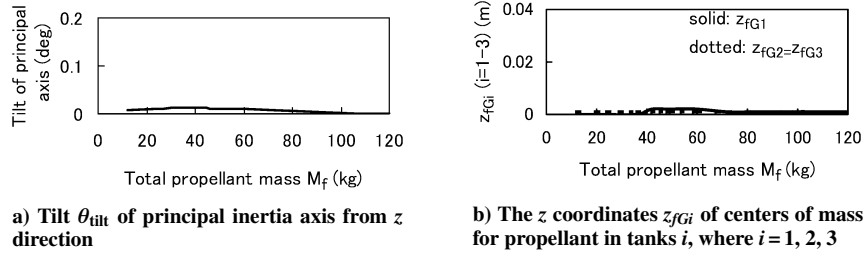


Fig. 8 Underestimated results when teardrop tanks are approximated by spherical tanks.

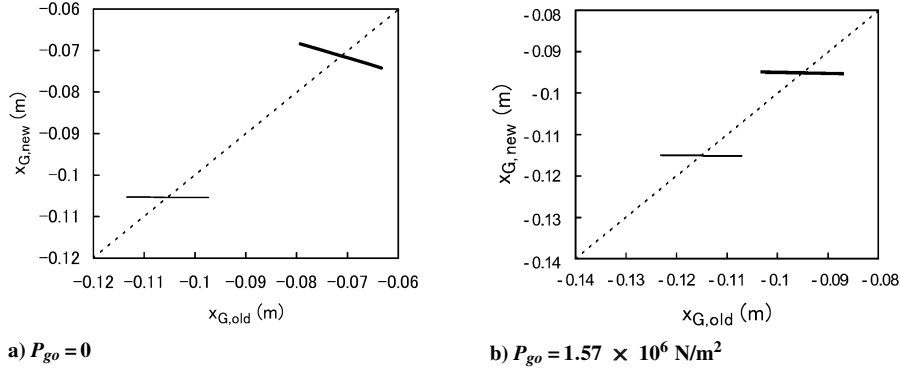


Fig. 9 Relation between the assumed and computed positions of the center of mass: —, $M_f = 60$ kg and —, $M_f = 12$ kg.

$p_{g0} = 1.57 \times 10^6$ N/m². 2) For the case of $p_{g0} = 0$, the magnitude of dx_G/dM_f changes almost discontinuously at the critical total propellant mass $M_{f,cr}$. To examine the physical meaning of these results, examples for the relation between the assumed and computed positions $x_{G,old}$ and $x_{G,new}$ of the center of mass are shown in Fig. 9. The points where $x_{G,old} = x_{G,new}$ is satisfied give the required solutions shown in Figs. 4a and 5a. For the case of $p_{g0} = 0$ and $M_f > M_{f,cr}$ (thick solid line in Fig. 9a), no tank is empty, so that the propellant migrates from tank 1 to tanks 2 and 3 due to the movement of the center of mass of the whole satellite–liquid system. Therefore, $x_{G,new}$ increases when $x_{G,old}$ is decreased, exhibiting the strong restoring effect on the position of the center of mass. For the other cases, the propellant migration among the tanks does not occur because tank 1 is empty or the propellant migration is effectively controlled by the initial gas pressure. Therefore, $x_{G,new}$ remains almost constant when $x_{G,old}$ is decreased, which reflects the weak restoring effect on the position of the center of mass. Thus, the relation between $x_{G,old}$ and $x_{G,new}$ exhibits a different tendency depending on the presence or absence of the propellant migration among the tanks. Results 1 and 2 mentioned earlier originate in the propellant migration among the tanks, which occurs when $p_{g0} = 0$ and $M_f > M_{f,cr}$.

To examine the influence of the difference among the gas temperatures in the tanks on the results, a computation was conducted using the state equations for the gas before and after the propellant migration:

$$p_{g0}(v_t - \rho^{-1} \frac{1}{3} M_f) = n_0 R T_{g0} \quad (15)$$

$$p_{gi}(v_t - \rho^{-1} M_{fi}) = n_0 R T_{gi} \quad (16)$$

where R is the gas constant, that is, $R = 8.31$ N·m/mol·K. Temperature conditions $T_{g0} = T_{g2} = T_{g3} = 273$ K and $T_{g1} = 323$ K were given to model a case in which the temperature difference promotes the propellant migration. From Eqs. (15) and (16), p_{gi} can be determined as

$$p_{gi} = \frac{p_{g0}(v_t - \rho^{-1} \frac{1}{3} M_f) T_{gi}}{(v_t - \rho^{-1} M_{fi}) T_{g0}} \quad (17)$$

When Eq. (11) is replaced with Eq. (17), the iterative procedures explained in the preceding section can be applied. The numerical

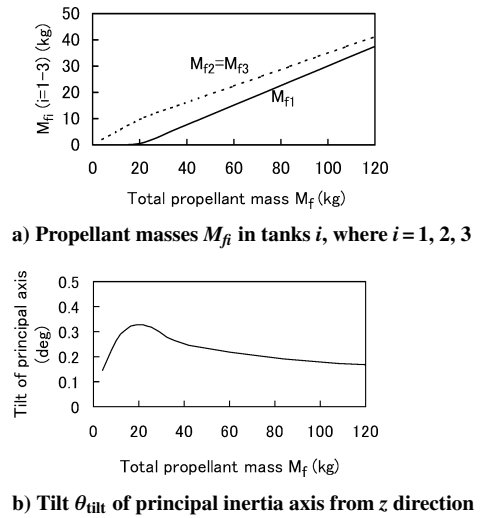
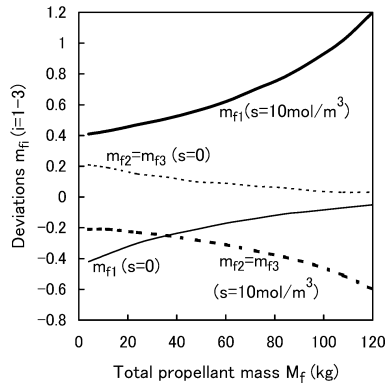


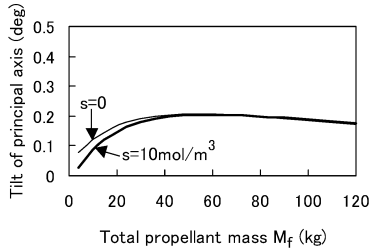
Fig. 10 Numerical results when temperature difference is given, $p_{g0} = 1.57 \times 10^6$ N/m².

results are presented in Fig. 10. It can be seen from the comparison between Fig. 10a and Fig. 5b that the critical total propellant mass $M_{f,cr}$ is increased from 2 to 20 kg by the temperature difference. Furthermore, comparison of Fig. 10b with Fig. 5c shows that the maximum tilt of the principal inertia axis is increased from 0.2 to 0.32 deg. However, $M_{f,cr}$ and the maximum tilt remain smaller than their uncontrolled values 40 kg and 0.42 deg for $p_{g0} = 0$ shown in Figs. 6 and 7, respectively, for the considerable magnitude of the temperature difference. In our project, the difference among temperatures of the tanks due to solar heating effects is reduced by spinning and enclosing the tanks with multilayer insulation. Therefore, the effectiveness of this propellant migration control method was examined assuming that the rotational imbalance effect due to the detachment of the object of not negligibly small mass compared with the main body is predominant to the thermal effects.

To apply the proposed method, a pressurant whose solubility in the propellant is very low is required. An example here considers hydrazine propellant and helium pressurant. However, examination



a) Deviations $m_{fi} \equiv M_{fi} - (1/3)M_f$ of propellant masses M_{fi} in tanks i , where $i = 1, 2, 3$, from their mean value



b) Tilt θ_{tilt} of principal inertia axis from z direction

Fig. 11 Numerical results when solubility of pressurant is considered, $p_{g0} = 1.57 \times 10^6 \text{ N/m}^2$.

of the influence of the solubility on the results is worthwhile for practical applications. To examine the influence, a computation was conducted using the state equations for the gas before and after the liquid migration:

$$p_{g0}(v_t - \rho^{-1} \frac{1}{3} M_f) = n_0 RT_{g0} \quad (18)$$

$$p_{gi} v_{gi} = [n_0 - s(p_{gi}/10130)(v_t - v_{gi})] RT_{g0} \quad (19)$$

where s is the solubility per unit volume of the propellant under the gas pressure equal to 10,130 N/m². From Eqs. (18) and (19), p_{gi} can be determined as

$$p_{gi} = \frac{p_{g0}(v_t - \rho^{-1} \frac{1}{3} M_f)}{v_{gi} + (1/10130)s(v_t - v_{gi}) RT_{g0}} \quad (20)$$

When Eq. (11) is replaced with Eq. (20), the present iterative procedures can be applied. The numerical results are presented in Fig. 11. The deviations $m_{fi} \equiv M_{fi} - (1/3)M_f$ of propellant masses M_{fi} in tanks i , where $i = 1, 2, 3$, are shown in Fig. 11a to show clearly the difference between the results for the following discussion. For the positive solubility, $M_{f2}(= M_{f3})$ is smaller than M_{f1} , in contrast to the case of the zero solubility. Therefore, the critical total propellant mass for the positive solubility is defined as the total propellant mass below which $M_{f2}(= M_{f3})$ is zero. When M_f is very small, $M_{f2}(= M_{f3})$ for the positive solubility is larger than M_{f1} for the zero solubility. Therefore, the critical total propellant mass is smaller for the positive solubility than for the zero solubility. As a result of this, the tilt of the principal inertia axis becomes smaller for the positive solubility than for the zero solubility, as can be seen from

Fig. 11b. When the solubility is zero, the relation $M_{f1} < M_{f2} = M_{f3}$ readily indicates that $v_{g1} > v_{g2} = v_{g3}$, that is, $p_{g1} < p_{g2} = p_{g3}$. This relation for the gas pressures is required to assure the effectiveness of the present propellant migration control method. Note that for the nonzero solubility, the required relation for the gas pressures may hold despite the relation $M_{f1} > M_{f2} = M_{f3}$ because a larger mass of gas dissolves in the propellant in tank 1 than in tank 2 or tank 3 due to the larger mass of solvent.

Summary

When a teardrop tank system undergoes a rotational unbalance due to the detachment of an object from a spinning satellite, we encounter a problem that there exists a considerably large critical value of the total propellant mass at which some of the tanks empty and a large tilt of the principal inertia axis occurs. To solve this problem, a method is proposed that supplies pressurized gas to the ullage in each tank and confines the gas by closing the valves among the tanks. The effectiveness of the proposed method was confirmed by numerical computation. This computation requires multiloop iterative procedures for satisfying the continuity condition for the liquid pressure in the pipes connecting the tanks and determining the position of the center of mass of the whole satellite-liquid system. The controlling effects of the gas pressure on the critical total propellant mass and the tilt of the principal inertia axis were illustrated and discussed.

In this practical example, taking into account the presence of the conical parts of the teardrop tanks is obligatory to avoid underestimating the tilt of the principal inertia axis, and the curvatures of the circular cylindrical liquid surfaces should be taken into account because the tanks are confined in the satellite compactly and are close to each other.

Acknowledgments

The present study was motivated by the development of a lunar exploration satellite LUNAR-A, the mission of which is to detach objects every few weeks and send them to the moon for examination of physical conditions at various places on the lunar surface. The author is grateful to members associated with the LUNAR-A project.

References

- ¹Honma, M., and Horikawa, Y., "Spin Axis Tilt of Satellite Introduced by the Internal Fluid Migration," National Space Development Agency of Japan, TR-8, Tokyo, Jan. 1979.
- ²McIntyre, J. E., and Miyagi, M. I., "A General Stability Principle for Spinning Flexible Bodies with Application to the Propellant Migration-Wobble Amplification Effect," *ESA Symposium on Dynamics and Control of Non-Rigid Space Vehicles*, ESA, Paris, 1976, pp. 159-175.
- ³Oberg, D. J., and Misra, P., "Propellant Management Operations on GSTAR-III," AIAA Paper 93-1800, June 1993.
- ⁴Ducret, E., Le Moullec, L., Spencer, B., and Balaam, P., "Propellant Management Device Studies, Computational Methods and Neutral Buoyancy Tests," AIAA Paper 92-3611, July 1992.
- ⁵Jaekle, D. E., Jr., "Propellant Management Device Conceptual Design and Analysis," AIAA Paper 93-1970, June 1993.
- ⁶Chapter, J. J., and Rider, S. B., "Surface Tension Propellant Management System Computerized Flow Analysis," AIAA Paper 80-1098, June-July 1980.
- ⁷Utsumi, M., "Position of Propellant in Teardrop Tank Systems," *Journal of Spacecraft and Rockets*, Vol. 34, No. 6, 1997, pp. 799-804.

N. Gatsonis
Associate Editor